Northumbria Research Link

Citation: Thai, Huu-Tai, Vo, Thuc, Nguyen, Trung-Kien and Lee, Jaehong (2014) A nonlocal sinusoidal plate model for micro/nanoscale plates. Proceedings of the Institution of Mechanical Engineers, Part C: Journal of Mechanical Engineering Science, 228 (14). pp. 2652-2660. ISSN 0954-4062

Published by: SAGE Publications

URL: http://dx.doi.org/10.1177/0954406214521391 <http://dx.doi.org/10.1177/0954406214521391>

A nonlocal sinusoidal plate model for micro/nanoscale plates

Huu-Tai Thai [a,*], Thuc P. Vo [b], Trung-Kien Nguyen[c], Jaehong Lee[d]

[a] School of Civil and Environmental Engineering, The University of New South Wales, Sydney, NSW 2052, Australia

[b] Faculty of Engineering and Environment, Northumbria University, Newcastle upon Tyne, NE1 8ST, UK.

[c] Faculty of Civil Engineering and Applied Mechanics, University of Technical Education Ho Chi Minh City, 1 Vo Van Ngan Street, Thu Duc District, Ho Chi Minh City, Vietnam.

[d] Department of Architectural Engineering, Sejong University, 98 Kunja Dong, Kwangjin Ku, Seoul 143-747, Korea

Abstract

A nonlocal sinusoidal plate model for micro/nanoscale plates is developed based on Eringen's nonlocal elasticity theory and sinusoidal shear deformation plate theory. The small scale effect is considered in the former theory while the transverse shear deformation effect is included in the latter theory. The proposed model accounts for sinusoidal variations of transverse shear strains through the thickness of the plate, and satisfies the stress-free boundary conditions on the plate surfaces, thus a shear correction factor is not required. Equations of motion and boundary conditions are derived from Hamilton's principle. Analytical solutions for bending, buckling, and vibration of simply supported plates are presented, and the obtained results are compared with the existing solutions. The effects of small scale and shear deformation on the responses of the micro/nanoscale plates are investigated.

Keywords: Sinusoidal shear deformation theory; Nonlocal elasticity theory; Bending; Buckling; Vibration

---

* Corresponding author. Tel.: + 61 2 9385 5029.
E-mail address: t.thai@unsw.edu.au (H.T. Thai).

1. Introduction

Nanostructures are being increasingly used in micro/nanoscale devices and systems such as biosensor, atomic force microscope, micro-electro-mechanical systems (MEMS), and nano-electro-mechanical systems (NEMS) due to their superior mechanical and electronic properties [1]. In such applications, small scale effects are experimentally observed [2-4]. It was found that when the thickness of these structures is close to the internal material length scale parameter, such effects are significant and have to be taken into account when studying their behavior. Conventional plate models based on classical continuum theories are not capable of describing such effects due to the lack of material length scale parameters. This motivated many researchers to develop plate models based on size-dependent continuum theories which account for the small scale effects. The nonlocal elasticity theory initiated by Eringen [5-7] is one of the promising size-dependent continuum theories. Unlike the classical continuum theories which assume that the stress at a point is a function of strain at that point, the nonlocal elasticity theory assumes that the stress at a point is a function of strains at all points in the continuum. In this way, the small scale effects are included through the use of constitutive equations.

Based on the nonlocal elasticity theory, a number of paper have been published in the last four years, attempting to develop nonlocal plate models and apply them to analyze the bending [8-12], buckling [13-21], and vibration [22-31] responses of nanoplates. All of these models were based on Kirchhoff plate theory [8, 12, 14-19, 22-27], Mindlin plate theory [9, 11, 20, 28-30], and Reddy plate theory [10, 13, 31]. It should be noted that the Kirchhoff plate theory (KPT) is only applicable for thin plates. However, it underestimates deflection and overestimates buckling load as well as natural frequency of moderately thick plates where the transverse shear deformation effects are significant. The Mindlin plate theory

(MPT) gives accurate results for thin to moderately thick plates, but it requires a shear correction factor to compensate for the difference between the actual stress state and the constant stress state due to a constant shear strain assumption through the thickness. The Reddy plate theory (RPT) provides a better prediction of response of thick plate and does not require a shear correction factor, but its equations of motion are more complicated than those of MPT.

The sinusoidal shear deformation theory of Touratier [32] is based on the assumption that the transverse shear stress vanishes on the top and bottom surfaces of the beam and is nonzero elsewhere. Thus there is no need to use shear correction factors as in the case of MPT. This theory was successfully applied to laminate plates [33] and functionally graded sandwich plates [34-36]. Therefore, it is useful to extend the application of this theory to the micro/nanoscale plates by accounting for the small scale effects. The aim of this paper is to extend the sinusoidal shear deformation theory of Touratier [32] to the micro/nanoscale plates. Equations of motion and boundary conditions are derived from Hamilton's principle based on the nonlocal constitutive relations of Eringen. Analytical solutions for deflection, buckling load, and natural frequency are presented for simply supported plates, and the obtained results are compared with the existing solutions to verify the accuracy of the present model.

2. Nonlocal plate model

2.1. Kinematics

The displacement field of the sinusoidal shear deformation theory is chosen based on the assumption that the transverse shear stress vanishes on the top and bottom surfaces of the beam and is nonzero elsewhere. The displacement field is given as [32]

$$u_1(x,y,z,t) = u(x,y,t) - z\frac{\partial w}{\partial x} + \frac{h}{\pi}\sin\left(\frac{\pi z}{h}\right)\varphi_x$$
$$u_2(x,y,z,t) = v(x,y,t) - z\frac{\partial w}{\partial y} + \frac{h}{\pi}\sin\left(\frac{\pi z}{h}\right)\varphi_y \quad (1)$$
$$u_3(x,y,z,t) = w(x,y,t)$$

where (u, v, w) are the displacements at a point on the middle plane of the plate along the coordinates (x, y, z); φ_x and φ_y are the rotation of the middle surface along the x and y directions, respectively; and h is the plate thickness.

The linear strain expressions associated with the displacement field in Eq. (1) are:

$$\varepsilon_x = \frac{\partial u}{\partial x} - z\frac{\partial^2 w}{\partial x^2} + \frac{h}{\pi}\sin\left(\frac{\pi z}{h}\right)\frac{\partial \varphi_x}{\partial x} \quad (2a)$$

$$\varepsilon_y = \frac{\partial u}{\partial y} - z\frac{\partial^2 w}{\partial y^2} + \frac{h}{\pi}\sin\left(\frac{\pi z}{h}\right)\frac{\partial \varphi_y}{\partial y} \quad (2b)$$

$$\gamma_{xy} = \frac{\partial u}{\partial y} + \frac{\partial v}{\partial x} - 2z\frac{\partial^2 w}{\partial x \partial y} + \frac{h}{\pi}\sin\left(\frac{\pi z}{h}\right)\left(\frac{\partial \varphi_x}{\partial y} + \frac{\partial \varphi_y}{\partial x}\right) \quad (2c)$$

$$\gamma_{xz} = \cos\left(\frac{\pi z}{h}\right)\varphi_x \quad (2d)$$

$$\gamma_{yz} = \cos\left(\frac{\pi z}{h}\right)\varphi_y \quad (2e)$$

It can be observed from Eqs. (2d) and (2e) that the transverse shear strains (γ_{xz}, γ_{yz}) are zero at the top ($z = h/2$) and bottom ($z = -h/2$) surfaces of the plate, thus satisfying the traction free conditions for (σ_{xz}, σ_{yz}).

2.2. Equations of motion

Hamilton's principle is used herein to derive the equations of motion. The principle can be stated in analytical form as

$$0 = \int_0^T \left(\delta U - \delta K\right) dt \tag{3}$$

where δU is the variation of strain energy; and δK is the variation of kinetic energy. The variation of strain energy of the plate is calculated by

$$\begin{aligned}
\delta U &= \int_A \int_{-h/2}^{h/2} \left(\sigma_x \delta\varepsilon_x + \sigma_y \delta\varepsilon_y + \sigma_{xy}\delta\gamma_{xy} + \sigma_{xz}\delta\gamma_{xz} + \sigma_{yz}\delta\gamma_{yz}\right) dAdz \\
&= \int_A \left[N_x \frac{\partial \delta u}{\partial x} - M_x \frac{\partial^2 \delta w}{\partial x^2} + P_x \frac{\partial \delta\varphi_x}{\partial x} + N_y \frac{\partial \delta v}{\partial y} - M_y \frac{\partial^2 \delta w}{\partial y^2} + P_y \frac{\partial \delta\varphi_y}{\partial y} \right. \\
&\quad \left. + N_{xy}\left(\frac{\partial \delta u}{\partial y} + \frac{\partial \delta v}{\partial x}\right) - 2M_{xy}\frac{\partial^2 \delta w}{\partial x \partial y} + P_{xy}\left(\frac{\partial \delta\varphi_x}{\partial y} + \frac{\partial \delta\varphi_y}{\partial x}\right) + Q_{xz}\delta\varphi_x + Q_{yz}\delta\varphi_y \right] dA
\end{aligned} \tag{4}$$

where N, M, P, and Q are the stress resultants defined as

$$N_i = \int_{-h/2}^{h/2} \sigma_i dz, \left(i = x, y, xy\right) \tag{5a}$$

$$M_i = \int_{-h/2}^{h/2} z\sigma_i dz, \left(i = x, y, xy\right) \tag{5b}$$

$$P_i = \int_{-h/2}^{h/2} \frac{h}{\pi} \sin\left(\frac{\pi z}{h}\right) \sigma_i dz, \left(i = x, y, xy\right) \tag{5c}$$

$$Q_i = \int_{-h/2}^{h/2} \cos\left(\frac{\pi z}{h}\right) \sigma_i dz, \left(i = xz, yz\right) \tag{5d}$$

The variation of kinetic energy of the plate can be written as

$$\begin{aligned}
\delta K &= \int_A \int_{-h/2}^{h/2} \left(\dot{u}_1 \delta\dot{u}_1 + \dot{u}_2 \delta\dot{u}_2 + \dot{u}_3 \delta\dot{u}_3\right) \rho dAdz \\
&= \int_A \left[I_0\left(\dot{u}\delta\dot{u} + \dot{v}\delta\dot{v} + \dot{w}\delta\dot{w}\right) + I_2\left(\frac{\partial \dot{w}}{\partial x}\frac{\partial \delta\dot{w}}{\partial x} + \frac{\partial \dot{w}}{\partial y}\frac{\partial \delta\dot{w}}{\partial y}\right) \right. \\
&\quad \left. - J_2\left(\frac{\partial \dot{w}}{\partial x}\delta\dot{\varphi}_x + \frac{\partial \dot{w}}{\partial y}\delta\dot{\varphi}_y + \dot{\varphi}_x \frac{\partial \delta\dot{w}}{\partial x} + \dot{\varphi}_y \frac{\partial \delta\dot{w}}{\partial y}\right) + K_2\left(\dot{\varphi}_x \delta\dot{\varphi}_x + \dot{\varphi}_y \delta\dot{\varphi}_y\right) \right] dA
\end{aligned} \tag{6}$$

where dot-superscript convention indicates the differentiation with respect to the time variable t; ρ is the mass density; and $\left(I_0, I_2, J_2, K_2\right)$ are the mass inertias defined as

$$I_0 = \int_{-h/2}^{h/2} \rho dz = \rho h \tag{7a}$$

$$I_2 = \int_{-h/2}^{h/2} \rho z^2 dz = \frac{\rho h^3}{12} \tag{7b}$$

$$J_2 = \int_{-h/2}^{h/2} \rho \frac{zh}{\pi} \sin\left(\frac{\pi z}{h}\right) dz = \frac{2\rho h^3}{\pi^3} \tag{7c}$$

$$K_2 = \int_{-h/2}^{h/2} \rho \left[\frac{h}{\pi} \sin\left(\frac{\pi z}{h}\right)\right]^2 dz = \frac{\rho h^3}{2\pi^2} \tag{7d}$$

Substituting the expressions for δU and δK from Eqs. (4) and (6) into Eq. (3) and integrating by parts, and collecting the coefficients of δu, δv, δw, $\delta \varphi_x$, and $\delta \varphi_y$, the following equations of motion are obtained:

$$\delta u: \ \frac{\partial N_x}{\partial x} + \frac{\partial N_{xy}}{\partial y} = I_0 \ddot{u} \tag{8a}$$

$$\delta v: \ \frac{\partial N_{xy}}{\partial x} + \frac{\partial N_y}{\partial y} = I_0 \ddot{v} \tag{8b}$$

$$\delta w: \frac{\partial^2 M_x}{\partial x^2} + 2\frac{\partial^2 M_{xy}}{\partial x \partial y} + \frac{\partial^2 M_y}{\partial y^2} + q + \tilde{N} = I_0 \ddot{w} - I_2 \nabla^2 \ddot{w} + J_2\left(\frac{\partial \ddot{\varphi}_x}{\partial x} + \frac{\partial \ddot{\varphi}_y}{\partial y}\right) \tag{8c}$$

$$\delta \varphi_x: \frac{\partial P_x}{\partial x} + \frac{\partial P_{xy}}{\partial y} - Q_{xz} = K_2 \ddot{\varphi}_x - J_2 \frac{\partial \ddot{w}}{\partial x} \tag{8d}$$

$$\delta \varphi_y: \frac{\partial P_{xy}}{\partial x} + \frac{\partial P_y}{\partial y} - Q_{yz} = K_2 \ddot{\varphi}_y - J_2 \frac{\partial \ddot{w}}{\partial y} \tag{8e}$$

The boundary conditions are of the forms

$$\delta u: 0 = N_x n_x + N_{xy} n_y \tag{9a}$$

$$\delta v: 0 = N_{xy} n_x + N_y n_y \tag{9b}$$

$$\delta w: 0 = V_x n_x + V_y n_y + \frac{\partial M_{ns}}{\partial s} \tag{9c}$$

$$\delta\varphi_x : 0 = P_x n_x + P_{xy} n_y \tag{9d}$$

$$\delta\varphi_y : 0 = P_{xy} n_x + P_y n_y \tag{9e}$$

$$\frac{\partial \delta w}{\partial n} : 0 = M_{nn} \tag{9f}$$

where

$$V_x = \frac{\partial M_x}{\partial x} + \frac{\partial M_{xy}}{\partial y} + N_x^0 \frac{\partial w}{\partial x} + N_{xy}^0 \frac{\partial w}{\partial y} + I_2 \frac{\partial \ddot{w}}{\partial x} - J_2 \ddot{\varphi}_x \tag{10a}$$

$$V_y = \frac{\partial M_y}{\partial y} + \frac{\partial M_{xy}}{\partial x} + N_{xy}^0 \frac{\partial w}{\partial x} + N_y^0 \frac{\partial w}{\partial y} + I_2 \frac{\partial \ddot{w}}{\partial y} - J_2 \ddot{\varphi}_y \tag{10b}$$

$$M_{ns} = \left(M_y - M_x\right) n_x n_y + M_{xy}\left(n_x^2 - n_y^2\right),\ M_{nn} = M_x n_x^2 + M_y n_y^2 + 2M_{xy} n_x n_y \tag{10c}$$

2.3. Constitutive relations

The nonlocal theory assumes that the stress at a point depends not only on the strain at that point but also on strains at all other points of the body. According to Eringen [5-7], the nonlocal stress tensor σ at a point is expressed as

$$\left(1 - \mu\nabla^2\right)\sigma = \tau \quad \text{or} \quad \Re\left(\sigma\right) = \tau \tag{11}$$

where ∇^2 is the Laplacian operator in two-dimensional Cartesian coordinate system; τ is the classical stress tensor at a point related to the strain by the Hooke's law; $\Re = 1 - \mu\nabla^2$ is a linear differential operator; and $\mu = (e_0 a)^2$ is the nonlocal parameter which incorporates the small scale effect, a is the internal characteristic length and e_0 is a constant appropriate to each material. The nonlocal parameter depends on the boundary conditions, chirality, mode shapes, number of walls, and type of motion [37]. So far, there is no rigorous study made on estimating the value of the nonlocal parameter. It is suggested that the value of nonlocal parameter can be determined by experiment or by conducting a comparison of dispersion curves from the nonlocal continuum mechanics and molecular dynamics simulation [38-40]. For an isotropic micro/nanoscale plate, the nonlocal constitutive relation in Eq. (11) takes the following forms [29, 31, 41-42]

$$\begin{Bmatrix} \sigma_x \\ \sigma_y \\ \sigma_{xy} \\ \sigma_{yz} \\ \sigma_{xz} \end{Bmatrix} - \mu\nabla^2 \begin{Bmatrix} \sigma_x \\ \sigma_y \\ \sigma_{xy} \\ \sigma_{yz} \\ \sigma_{xz} \end{Bmatrix} = \frac{E}{1-\nu^2} \begin{bmatrix} 1 & \nu & 0 & 0 & 0 \\ \nu & 1 & 0 & 0 & 0 \\ 0 & 0 & \frac{(1-\nu)}{2} & 0 & 0 \\ 0 & 0 & 0 & \frac{(1-\nu)}{2} & 0 \\ 0 & 0 & 0 & 0 & \frac{(1-\nu)}{2} \end{bmatrix} \begin{Bmatrix} \varepsilon_x \\ \varepsilon_y \\ \gamma_{xy} \\ \gamma_{yz} \\ \gamma_{xz} \end{Bmatrix} \tag{12}$$

where E and ν are the elastic modulus and Poisson's ratio, respectively. Using Eqs. (2), (12) and (5), the stress resultants can be expressed in terms of displacements as

$$\begin{Bmatrix} N_x \\ N_y \\ N_{xy} \end{Bmatrix} - \mu\nabla^2 \begin{Bmatrix} N_x \\ N_y \\ N_{xy} \end{Bmatrix} = A \begin{bmatrix} 1 & \nu & 0 \\ \nu & 1 & 0 \\ 0 & 0 & \frac{1-\nu}{2} \end{bmatrix} \begin{Bmatrix} \frac{\partial u}{\partial x} \\ \frac{\partial v}{\partial y} \\ \frac{\partial u}{\partial y} + \frac{\partial v}{\partial x} \end{Bmatrix} \tag{13a}$$

$$\begin{Bmatrix} M_x \\ M_y \\ M_{xy} \end{Bmatrix} - \mu\nabla^2 \begin{Bmatrix} M_x \\ M_y \\ M_{xy} \end{Bmatrix} = D \begin{bmatrix} 1 & \nu & 0 \\ \nu & 1 & 0 \\ 0 & 0 & \frac{1-\nu}{2} \end{bmatrix} \begin{Bmatrix} -\frac{\partial^2 w}{\partial x^2} \\ -\frac{\partial^2 w}{\partial y^2} \\ -2\frac{\partial^2 w}{\partial x \partial y} \end{Bmatrix} + F \begin{bmatrix} 1 & \nu & 0 \\ \nu & 1 & 0 \\ 0 & 0 & \frac{1-\nu}{2} \end{bmatrix} \begin{Bmatrix} \frac{\partial \varphi_x}{\partial x} \\ \frac{\partial \varphi_y}{\partial y} \\ \frac{\partial \varphi_x}{\partial y} + \frac{\partial \varphi_y}{\partial x} \end{Bmatrix} \tag{13b}$$

$$\begin{Bmatrix} P_x \\ P_y \\ P_{xy} \end{Bmatrix} - \mu\nabla^2 \begin{Bmatrix} P_x \\ P_y \\ P_{xy} \end{Bmatrix} = F \begin{bmatrix} 1 & \nu & 0 \\ \nu & 1 & 0 \\ 0 & 0 & \frac{1-\nu}{2} \end{bmatrix} \begin{Bmatrix} -\frac{\partial^2 w}{\partial x^2} \\ -\frac{\partial^2 w}{\partial y^2} \\ -2\frac{\partial^2 w}{\partial x \partial y} \end{Bmatrix} + H \begin{bmatrix} 1 & \nu & 0 \\ \nu & 1 & 0 \\ 0 & 0 & \frac{1-\nu}{2} \end{bmatrix} \begin{Bmatrix} \frac{\partial \varphi_x}{\partial x} \\ \frac{\partial \varphi_y}{\partial y} \\ \frac{\partial \varphi_x}{\partial y} + \frac{\partial \varphi_y}{\partial x} \end{Bmatrix} \tag{13c}$$

$$\begin{Bmatrix} Q_{xz} \\ Q_{yz} \end{Bmatrix} - \mu\nabla^2 \begin{Bmatrix} Q_{xz} \\ Q_{yz} \end{Bmatrix} = A^s \begin{bmatrix} 1 & 0 \\ 0 & 1 \end{bmatrix} \begin{Bmatrix} \varphi_x \\ \varphi_y \end{Bmatrix} \tag{13d}$$

where

$$(A, D, F, H) = \frac{E}{1-\nu^2}\left(h, \frac{h^3}{12}, \frac{2h^3}{\pi^3}, \frac{h^3}{2\pi^2}\right), \quad A^s = \frac{Eh}{4(1+\nu)} \tag{14}$$

2.4. Equations of motion in terms of displacements

The nonlocal equations of motion of the present theory can be expressed in terms of generalized displacements $(u, v, w, \varphi_x, \varphi_y)$ by applying linear differential operator $\Re$

on Eq. (8)

$$A\left(\frac{\partial^2 u}{\partial x^2}+\frac{1-\nu}{2}\frac{\partial^2 u}{\partial y^2}+\frac{1+\nu}{2}\frac{\partial^2 v}{\partial x\partial y}\right)=I_0\left(\ddot{u}-\mu\nabla^2\ddot{u}\right) \tag{15a}$$

$$A\left(\frac{\partial^2 v}{\partial y^2}+\frac{1-\nu}{2}\frac{\partial^2 v}{\partial x^2}+\frac{1+\nu}{2}\frac{\partial^2 u}{\partial x\partial y}\right)=I_0\left(\ddot{v}-\mu\nabla^2\ddot{v}\right) \tag{15b}$$

$$\begin{aligned}&-D\nabla^4 w+F\nabla^2\left(\frac{\partial\varphi_x}{\partial x}+\frac{\partial\varphi_y}{\partial y}\right)+q-\mu\nabla^2 q+\tilde{N}-\mu\nabla^2\tilde{N}\\&=I_0\left(\ddot{w}-\mu\nabla^2\ddot{w}\right)-I_2\left(\nabla^2\ddot{w}-\mu\nabla^4\ddot{w}\right)+J_2\left[\left(\frac{\partial\ddot{\varphi}_x}{\partial x}+\frac{\partial\ddot{\varphi}_y}{\partial y}\right)-\mu\nabla^2\left(\frac{\partial\ddot{\varphi}_x}{\partial x}+\frac{\partial\ddot{\varphi}_y}{\partial y}\right)\right]\end{aligned} \tag{15c}$$

$$\begin{aligned}&-F\nabla^2\frac{\partial w}{\partial x}+H\left(\frac{\partial^2\varphi_x}{\partial x^2}+\frac{1-\nu}{2}\frac{\partial^2\varphi_x}{\partial y^2}+\frac{1+\nu}{2}\frac{\partial^2\varphi_y}{\partial x\partial y}\right)-A^s\varphi_x\\&=K_2\left(\ddot{\varphi}_x-\mu\nabla^2\ddot{\varphi}_x\right)-J_2\left(\frac{\partial\ddot{w}}{\partial x}-\mu\nabla^2\frac{\partial\ddot{w}}{\partial x}\right)\end{aligned} \tag{15d}$$

$$\begin{aligned}&-F\nabla^2\frac{\partial w}{\partial y}+H\left(\frac{\partial^2\varphi_y}{\partial y^2}+\frac{1-\nu}{2}\frac{\partial^2\varphi_y}{\partial x^2}+\frac{1+\nu}{2}\frac{\partial^2\varphi_x}{\partial x\partial y}\right)-A^s\varphi_y\\&=K_2\left(\ddot{\varphi}_y-\mu\nabla^2\ddot{\varphi}_y\right)-J_2\left(\frac{\partial\ddot{w}}{\partial y}-\mu\nabla^2\frac{\partial\ddot{w}}{\partial y}\right)\end{aligned} \tag{15e}$$

Clearly, when the nonlocal effect is neglected (i.e. $\mu=0$), the present model recovers Touratier's sinusoidal shear deformation theory [32]. Also, the equations of motion of the nonlocal KPT can be obtained from Eq. (15) by setting the rotations (φ_x,φ_y) equal to zero. It is observed from Eq. (15) that the in-plane displacements (u,v) are uncoupled from the transverse displacements (w,φ_x,φ_y). Thus, the equations of motion for the transverse response of the plate are reduced to Eqs. (15c)-(15e).

3. Analytical solutions

Consider a simply supported rectangular plate with length L and width b under transverse load q and in-plane load in two directions ($N_x^0 = \gamma_1 N_{cr}, N_y^0 = \gamma_2 N_{cr}, N_{xy}^0 = 0$). Based on the Navier approach, the following expansions of displacements are chosen to automatically satisfy the simply supported boundary conditions of plate

$$\begin{aligned}
\varphi_x(x, y, t) &= \sum_{m=1}^{\infty}\sum_{n=1}^{\infty} X_{mn} \cos\alpha x \sin\beta y e^{i\omega t} \\
\varphi_y(x, y, t) &= \sum_{m=1}^{\infty}\sum_{n=1}^{\infty} Y_{mn} \sin\alpha x \cos\beta y e^{i\omega t} \\
w(x, y, t) &= \sum_{m=1}^{\infty}\sum_{n=1}^{\infty} W_{mn} \sin\alpha x \sin\beta y e^{i\omega t}
\end{aligned} \tag{16}$$

where $i = \sqrt{-1}$, $\alpha = m\pi / L$, $\beta = n\pi / b$, (X_{mn}, Y_{mn}, W_{mn}) are coefficients, and ω is the natural frequency. The transverse load q is also expanded in the double-Fourier sine series as

$$q(x, y) = \sum_{m=1}^{\infty}\sum_{n=1}^{\infty} Q_{mn} \sin\alpha x \sin\beta y \tag{17}$$

where

$$Q_{mn} = \frac{4}{Lb}\int_0^L\int_0^b q(x, y)\sin\alpha x \sin\beta y dxdy \tag{18}$$

The coefficients Q_{mn} are given below for some typical loads:

$$Q_{mn} = \begin{cases} q_0 & \text{for sinusoidal load of intensity } q_0 \\ \dfrac{16q_0}{mn\pi^2} & \text{for uniform load of intensity } q_0 \\ \dfrac{4Q_0}{Lb}\sin\dfrac{m\pi}{2}\sin\dfrac{n\pi}{2} & \text{for point load } Q_0 \text{ at the center} \end{cases} \tag{19}$$

Substituting the expansions of (φ_x, φ_y, w) and q from Eqs. (16) and (17) into Eq. (15), the analytical solutions can be obtained from the following equations

$$\left(\begin{bmatrix} s_{11} & s_{12} & s_{13} \\ s_{12} & s_{22} & s_{23} \\ s_{13} & s_{23} & s_{33} + k\lambda \end{bmatrix} - \omega^2 \lambda \begin{bmatrix} m_{11} & 0 & m_{13} \\ 0 & m_{22} & m_{23} \\ m_{13} & m_{23} & m_{33} \end{bmatrix} \right) \begin{Bmatrix} X_{mn} \\ Y_{mn} \\ W_{mn} \end{Bmatrix} = \begin{Bmatrix} 0 \\ 0 \\ \lambda Q_{mn} \end{Bmatrix} \tag{20}$$

where

$$
\begin{aligned}
& s_{11} = A^s + H\left(\alpha^2 + \frac{1-\nu}{2}\beta^2\right), \; s_{22} = A^s + H\left(\beta^2 + \frac{1-\nu}{2}\alpha^2\right) \\
& s_{12} = H\alpha\beta\frac{1+\nu}{2}, \; s_{13} = -F\alpha\left(\alpha^2+\beta^2\right), \; s_{23} = -F\beta\left(\alpha^2+\beta^2\right) \\
& s_{33} = D\left(\alpha^2+\beta^2\right)^2, \; k = N_{cr}\left(\gamma_1\alpha^2+\gamma_2\beta^2\right), \; \lambda = 1+\mu\left(\alpha^2+\beta^2\right) \\
& m_{11} = K_2, \; m_{22} = K_2, \; m_{33} = I_0 + I_2\left(\alpha^2+\beta^2\right), \; m_{13} = -\alpha J_2, \; m_{23} = -\beta J_2
\end{aligned}
\tag{21}
$$

The analytical solution of the nonlocal KPT can be obtained from Eq. (20) by setting coefficients (X_{mn}, Y_{mn}) equal to zero. Thus, the deflection w, buckling load N_{cr}, and natural frequency ω of the KPT are expressed as

$$
w(x,y) = \sum_{m=1}^{\infty}\sum_{n=1}^{\infty}\frac{\lambda Q_{mn}}{D\left(\alpha^2+\beta^2\right)^2}\sin\alpha x\sin\beta y \tag{22a}
$$

$$
N_{cr} = -\frac{D\left(\alpha^2+\beta^2\right)^2}{\lambda\left(\gamma_1\alpha^2+\gamma_2\beta^2\right)} \tag{22b}
$$

$$
\omega^2 = \frac{D\left(\alpha^2+\beta^2\right)^2}{\lambda\left[I_0 + I_2\left(\alpha^2+\beta^2\right)\right]} \tag{22c}
$$

4. Numerical results

In this section, a simply supported nanoplate made of single-layered graphene sheet (SLGS) is considered. The geometric and mechanical properties of the SLGS are [43]: $E = 1.02$ TPa, $\nu = 0.16$, $\rho = 2,250$ kg/m^3, $h = 0.34$ nm. The fundamental frequency of simply-supported armchair and zigzag square SLGSs with different side lengths L are presented in Table 1. The values of nonlocal parameter e_0a of the simply-supported armchair and zigzag SLGSs are 1.16 nm and 1.19 nm, respectively. The obtained results are compared with those predicted by molecular dynamics (MD) simulation [38] which is one of the most widely used numerical methods related to the interaction between the atoms or molecules in a system. A good agreement between the results is observed for various sizes of the plate.

To further validate the accuracy of the present solutions, the obtained results are compared with those predicted by MPT in Table 2 for simply supported square plates with various values of side lengths L and nonlocal parameter $e_0a = 0$ to 2.0 nm. The reason for choosing these values is that e_0a should be smaller than 2.0 nm for a single-wall carbon nanotube as pointed out by Wang and Wang [44]. Since the maximum value of e_0a has not been exactly known for graphene sheet, it is assumed to be equal to that of the single-wall carbon nanotube. The shear correction factor used in MPT is taken as 5/6. The nondimensional deflection is obtained for the plate subjected to uniform loads, while the nondimensional critical buckling load is calculated for the plate subjected to biaxial compression. The nondimensional deflection $\bar{w}$, critical buckling load $\bar{N}$, and fundamental frequency $\bar{\omega}$ are defined by

$$\bar{w} = \frac{wEh^3}{q_0L^4}, \quad \bar{N} = \frac{N_{cr}L^2}{Eh^3}, \quad \bar{\omega} = \frac{\omega L^2}{h}\sqrt{\rho / E} \tag{23}$$

It can be seen that the present theory and MPT give almost identical results for all cases ranging from thin to thick plates confirming the accuracy of present solutions. It should be noted that the present theory does not require shear correction factors as in the case of MPT.

To illustrate the small scale effects on the responses of nanoplates, Figs. 1-3 plot the deflection, buckling load, and frequency ratios with respect to the size of a simply-supported plate. The value of nonlocal parameter e_0a of a simply-supported armchair nanoplate is 1.16 nm [38]. The deflection, buckling load, and frequency ratios are defined as the ratios of those predicted by the nonlocal theory to the correspondences obtained by the local theory (i.e., $e_0a = 0$). It can be seen that the deflection ratio is greater than unity, whereas the buckling load and frequency ratios are smaller than unity. It means that the local theory underestimates deflection (see Fig. 1) and overestimates buckling load (see Fig. 2) and natural frequency (see Fig. 3). This is due to the fact that the local theory ignores the small scale effect. In other words, the inclusion of the small scale effect leads to an increase in the deflection and a reduction of the buckling load and natural frequency. The small scale effect is significant for thick plates (i.e. the size of the plate is small) especially at the higher modes (see Figs. 2 and 3). However, it will diminish for very thin plates (i.e. the size of the plate is large).

In addition to the small scale effect, the present nonlocal plate model also accounts for the shear deformation effect. The effect of shear deformation on the deflection, buckling load, and natural frequency of a simply-supported nanoplate is illustrated in Figs. 4-6, respectively. The nonlocal parameter e_0a is taken as 1.16 nm [38]. In these figures, the deflection, buckling load, and frequency ratios are defined as the ratios of those obtained by the present nonlocal theory to the correspondences predicted by the nonlocal KPT where the shear deformation effect is omitted. It can be seen that the effect of shear deformation leads to an increase in the deflection and a reduction of the buckling load and natural frequency, and this effect is significant for thick plates especially at the higher modes (see Figs. 5 and 6). It means that the shear deformation effect makes the plate more flexible.

5. Conclusions

A nonlocal plate model for bending, buckling, and free vibration of micro/nanoscale plates is developed based on the nonlocal differential constitutive relations of Eringen.

Equations of motion and boundary conditions are derived from Hamilton's principle. Analytical solutions for bending, buckling, and free vibration of a simply supported plate are presented, and the obtained results are compared well with those generated by MD simulation and those predicted by the nonlocal MPT. As shown in this study, the effects of small scale and shear deformation are similar. The inclusion of small scale and shear deformation effects makes the plate more flexible, and consequently, leads to an increase in the deflection and a reduction of the buckling load and natural frequency. These effects are significant for thick plates especially at the higher modes, but they will diminish for very thin plates.

Acknowledgements

The third author gratefully acknowledges financial support from Vietnam National Foundation for Science and Technology Development (NAFOSTED) under Grant No. 107.02-2012.07, and from University of Technical Education Ho Chi Minh City.

References

1. Li X, Bhushan B, Takashima K, Baek CW and Kim YK. Mechanical characterization of micro/nanoscale structures for MEMS/NEMS applications using nanoindentation techniques. Ultramicroscopy. 2003; 97: 481-94.

2. Chong ACM, Yang F, Lam DCC and Tong P. Torsion and bending of micron-scaled structures. Journal of Materials Research. 2001; 16: 1052-8.

3. Fleck NA, Muller GM, Ashby MF and Hutchinson JW. Strain gradient plasticity: theory and experiment. Acta Metallurgica et Materialia. 1994; 42: 475-87.

4. Stolken JS and Evans AG. A microbend test method for measuring the plasticity length scale. Acta Materialia. 1998; 46: 5109-15.

5. Eringen AC. Nonlocal polar elastic continua. International Journal of Engineering Science. 1972; 10: 1-16.

6. Eringen AC. On differential equations of nonlocal elasticity and solutions of screw dislocation and surface waves. Journal of Applied Physics. 1983; 54: 4703-10.

7. Eringen AC and Edelen DGB. On nonlocal elasticity. International Journal of Engineering Science. 1972; 10: 233-48.

8. Duan WH and Wang CM. Exact solutions for axisymmetric bending of micro/nanoscale circular plates based on nonlocal plate theory. Nanotechnology. 2007; 18: 385704.

9. Lu P, Zhang PQ, Lee HP, Wang CM and Reddy JN. Non-local elastic plate theories. Proceedings of the Royal Society A: Mathematical, Physical and Engineering Science. 2007; 463: 3225-40.

10. Aghababaei R and Reddy JN. Nonlocal third-order shear deformation plate theory with application to bending and vibration of plates. Journal of Sound and Vibration. 2009; 326: 277-89.

11. Reddy JN. Nonlocal nonlinear formulations for bending of classical and shear deformation theories of beams and plates. International Journal of Engineering Science. 2010; 48: 1507-18.

12. Hui-Shen S. Nonlocal plate model for nonlinear analysis of thin films on elastic foundations in thermal environments. Composite Structures. 2011; 93: 1143-52.

13. Pradhan SC. Buckling of single layer graphene sheet based on nonlocal elasticity and higher order shear deformation theory. Physics Letters A. 2009; 373: 4182-8.

14. Murmu T and Pradhan SC. Buckling of biaxially compressed orthotropic plates at small scales. Mechanics Research Communications. 2009; 36: 933-8.

15. Pradhan SC and Murmu T. Small scale effect on the buckling of single-layered graphene sheets under biaxial compression via nonlocal continuum mechanics. Computational Materials Science. 2009; 47: 268-74.

16. Pradhan SC and Phadikar JK. Scale effect and buckling analysis of multilayered graphene sheets based on nonlocal continuum mechanics. Journal of Computational and Theoretical Nanoscience. 2010; 7: 1948-54.

17. Malekzadeh P, Setoodeh AR and Alibeygi Beni A. Small scale effect on the thermal buckling of orthotropic arbitrary straight-sided quadrilateral nanoplates embedded in an elastic medium. Composite Structures. 2011; 93: 2083-9.

18. Babaei H and Shahidi AR. Small-scale effects on the buckling of quadrilateral nanoplates based on nonlocal elasticity theory using the Galerkin method. Archive of Applied Mechanics. 2011; 81: 1051-62.

19. Aksencer T and Aydogdu M. Levy type solution method for vibration and buckling of nanoplates using nonlocal elasticity theory. Physica E: Low-dimensional Systems and Nanostructures. 2011; 43: 954-9.

20. Hashemi SH and Samaei AT. Buckling analysis of micro/nanoscale plates via nonlocal elasticity theory. Physica E: Low-dimensional Systems and Nanostructures. 2011; 43: 1400-4.

21. Narendar S. Buckling analysis of micro-/nano-scale plates based on two-variable refined plate theory incorporating nonlocal scale effects. Composite Structures. 2011; 93: 3093-103.

22. Pradhan SC and Phadikar JK. Small scale effect on vibration of embedded multilayered graphene sheets based on nonlocal continuum models. Physics Letters A. 2009; 373: 1062-9.

23. Murmu T and Pradhan SC. Small-scale effect on the free in-plane vibration of nanoplates by nonlocal continuum model. Physica E: Low-dimensional Systems and Nanostructures. 2009; 41: 1628-33.

24. Murmu T and Pradhan SC. Vibration analysis of nanoplates under uniaxial prestressed conditions via nonlocal elasticity. Journal of Applied Physics. 2009; 106: 104301.

25. Murmu T and Pradhan SC. Vibration analysis of nano-single-layered graphene sheets embedded in elastic medium based on nonlocal elasticity theory. Journal of Applied Physics. 2009; 105: 064319.

26. Wang CY, Murmu T and Adhikari S. Mechanisms of nonlocal effect on the vibration of nanoplates. Applied Physics Letters. 2011; 98: 153101.

27. Pradhan SC and Kumar A. Vibration analysis of orthotropic graphene sheets using nonlocal elasticity theory and differential quadrature method. Composite Structures. 2011; 93: 774-9.

28. Pradhan SC and Phadikar JK. Nonlocal elasticity theory for vibration of nanoplates. Journal of Sound and Vibration. 2009; 325: 206-23.

29. Ansari R, Arash B and Rouhi H. Vibration characteristics of embedded multi-layered graphene sheets with different boundary conditions via nonlocal elasticity. Composite Structures. 2011; 93: 2419-29.

30. Malekzadeh P, Setoodeh AR and Alibeygi Beni A. Small scale effect on the free vibration of orthotropic arbitrary straight-sided quadrilateral nanoplates. Composite Structures. 2011; 93: 1631-9.

31. Pradhan SC and Sahu B. Vibration of single layer graphene sheet based on nonlocal elasticity and higher order shear deformation theory. Journal of Computational and

Theoretical Nanoscience. 2010; 7: 1042-50.

32. Touratier M. An efficient standard plate theory. International Journal of Engineering Science. 1991; 29: 901-16.

33. Zenkour AM. Analytical solution for bending of cross-ply laminated plates under thermo-mechanical loading. Composite Structures. 2004; 65: 367-79.

34. Zenkour AM. A comprehensive analysis of functionally graded sandwich plates: Part 1-Deflection and stresses. International Journal of Solids and Structures. 2005; 42: 5224-42.

35. Zenkour AM. A comprehensive analysis of functionally graded sandwich plates: Part 2-Buckling and free vibration. International Journal of Solids and Structures. 2005; 42: 5243-58.

36. Zenkour AM. Generalized shear deformation theory for bending analysis of functionally graded plates. Applied Mathematical Modelling. 2006; 30: 67-84.

37. Arash B and Wang Q. A review on the application of nonlocal elastic models in modeling of carbon nanotubes and graphenes. Computational Materials Science. 2012; 51: 303-13.

38. Ansari R, Sahmani S and Arash B. Nonlocal plate model for free vibrations of single-layered graphene sheets. Physics Letters A. 2010; 375: 53-62.

39. Arash B and Ansari R. Evaluation of nonlocal parameter in the vibrations of single-walled carbon nanotubes with initial strain. Physica E: Low-dimensional Systems and Nanostructures. 2010; 42: 2058-64.

40. Narendar S, Roy Mahapatra D and Gopalakrishnan S. Prediction of nonlocal scaling parameter for armchair and zigzag single-walled carbon nanotubes based on molecular structural mechanics, nonlocal elasticity and wave propagation. International Journal of

Engineering Science. 2011; 49: 509-22.

41. Ansari R, Arash B and Rouhi H. Nanoscale vibration analysis of embedded multi-layered graphene sheets under various boundary conditions. Computational Materials Science. 2011; 50: 3091-100.

42. Ansari R, Rajabiehfard R and Arash B. Nonlocal finite element model for vibrations of embedded multi-layered graphene sheets. Computational Materials Science. 2010; 49: 831-8.

43. Kitipornchai S, He XQ and Liew KM. Continuum model for the vibration of multilayered graphene sheets. Physical Review B. 2005; 72: 075443.

44. Wang Q and Wang C. The constitutive relation and small scale parameter of nonlocal continuum mechanics for modelling carbon nanotubes. Nanotechnology. 2007; 18: 075702.

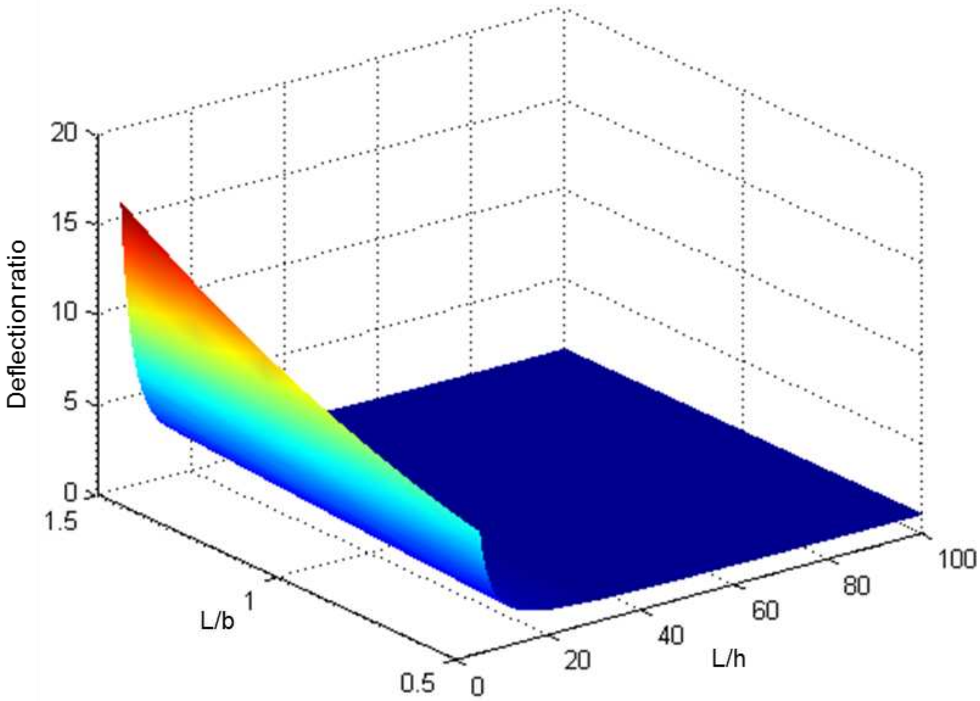

Fig. 1. Effect of small scale on deflection ratio of simply supported plates under sinusoidal load

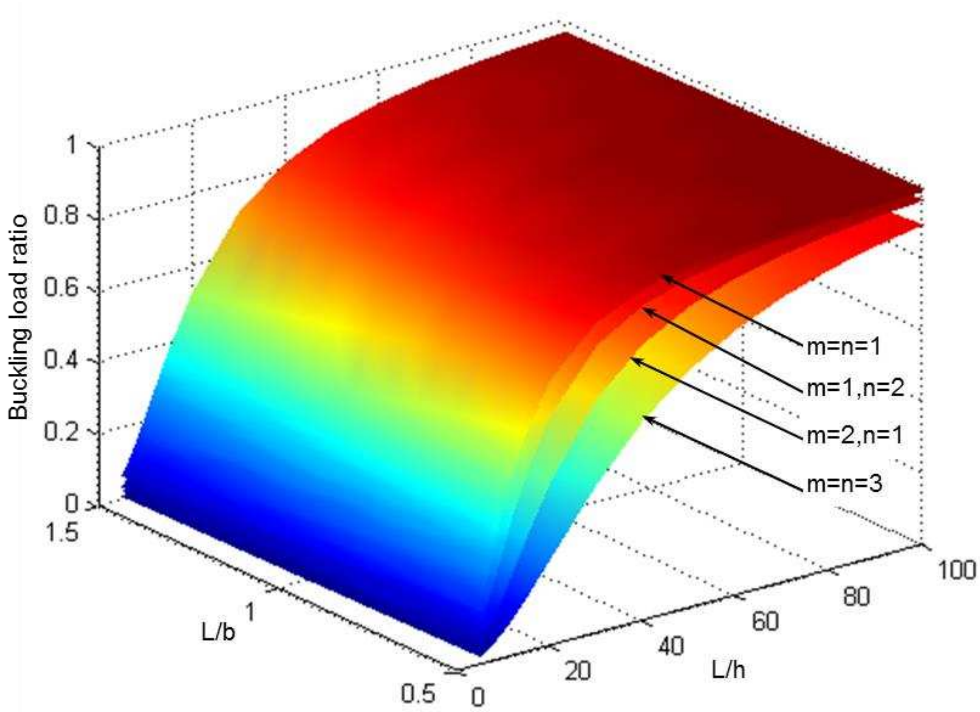

Fig. 2. Effect of small scale on buckling load ratio of simply supported plates under biaxial compression

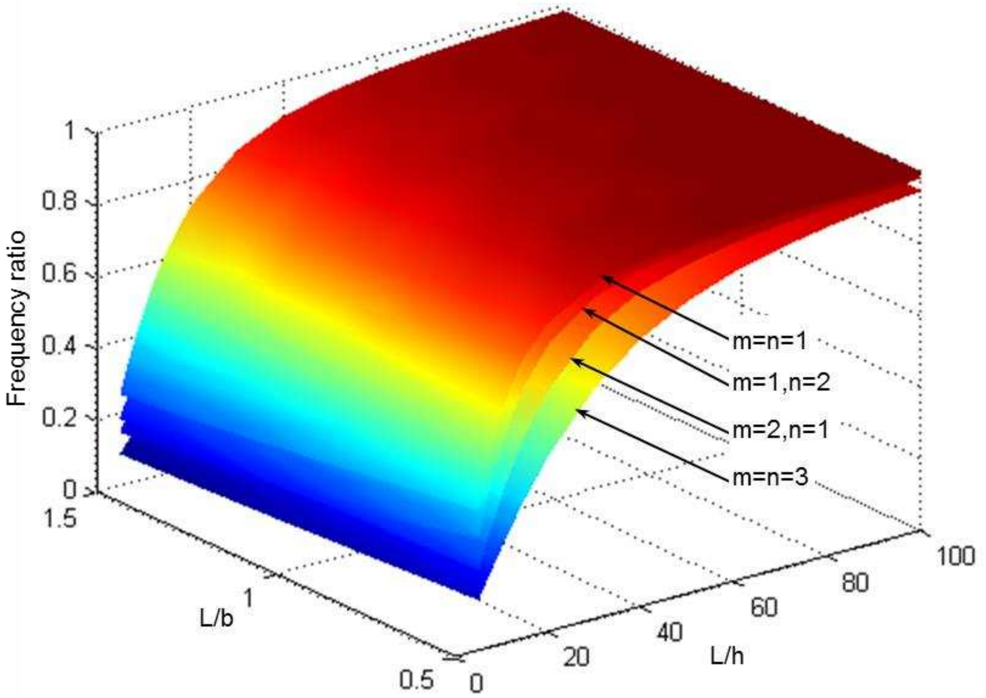

Fig. 3. Effect of small scale on frequency ratio of simply supported plates

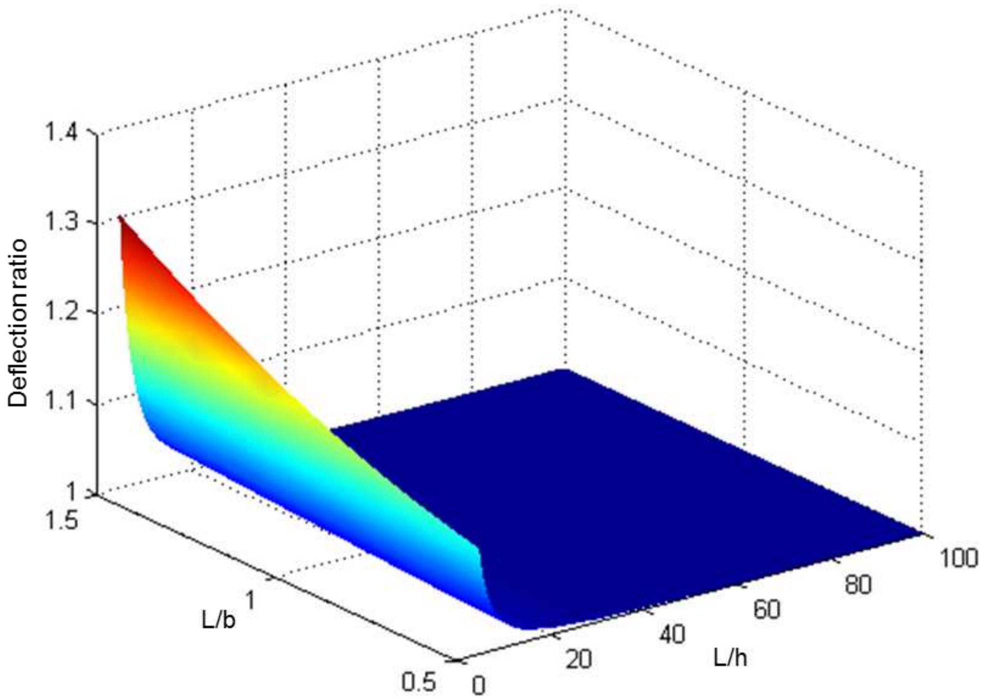

Fig. 4. Effect of shear deformation on deflection ratio of simply supported plates under sinusoidal load

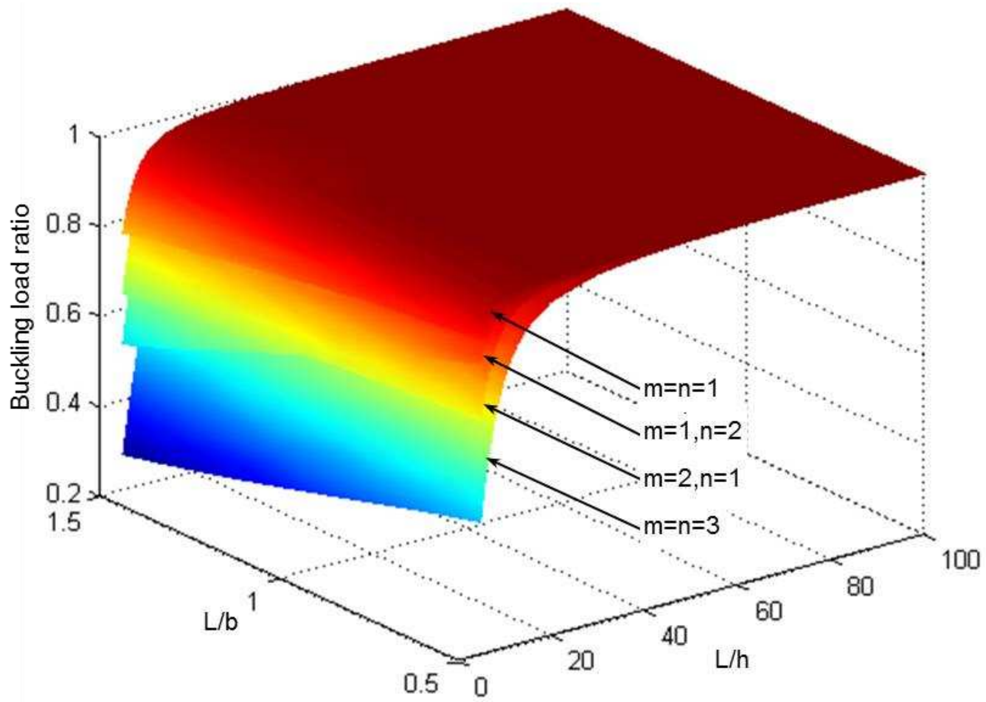

Fig. 5. Effect of shear deformation on buckling load ratio of simply supported plates under biaxial compression

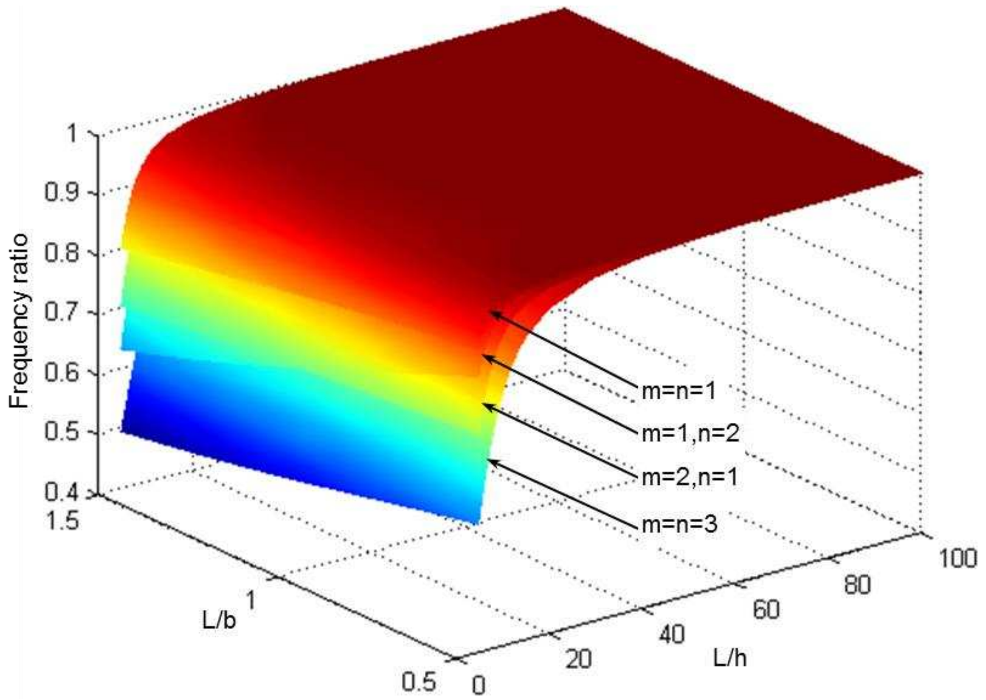

Fig. 6. Effect of shear deformation on frequency ratio of simply supported plates

Table 1. Fundamental frequency (THz) of simply support square SLGSs

L (nm)	Armchair SLGS, $e_oa = 1.16$ (nm)			Zigzag SLGS, $e_oa = 1.19$ (nm)		
	MD [38]	Present	Diff. (%)	MD [38]	Present	Diff. (%)
10	0.05950	0.05893	-0.96	0.05877	0.05861	-0.28
15	0.02779	0.02792	0.44	0.02739	0.02784	1.65
20	0.01581	0.01609	1.74	0.01575	0.01606	1.97
25	0.01000	0.01042	4.20	0.00998	0.01041	4.23
30	0.00707	0.00728	2.96	0.00707	0.00728	2.97
35	0.00530	0.00537	1.32	0.00530	0.00537	1.30
40	0.00410	0.00412	0.49	0.00410	0.00412	0.53
45	0.00326	0.00326	0.04	0.00326	0.00326	0.02
50	0.00262	0.00265	1.00	0.00262	0.00265	0.99

Table 2. Nondimensional deflection $\bar{w}$, critical buckling load $\bar{N}$, and fundamental frequency $\bar{\omega}$ of simply supported square plates

L/h	e_oa (nm)	Deflection $\bar{w}$		Buckling load $\bar{N}$		Frequency $\bar{\omega}$	
		MPT	Present	MPT	Present	MPT	Present
5	0	0.0557	0.0557	1.4210	1.4220	5.1759	5.1774
	0.5	0.1397	0.1398	0.5248	0.5252	3.1456	3.1465
	1.0	0.3918	0.3922	0.1815	0.1816	1.8497	1.8502
	1.5	0.8120	0.8128	0.0868	0.0869	1.2794	1.2797
	2.0	1.4002	1.4017	0.0502	0.0502	0.9726	0.9729
10	0	0.0496	0.0495	1.6124	1.6125	5.5997	5.5999
	0.5	0.0688	0.0688	1.1300	1.1301	4.6878	4.6880
	1.0	0.1264	0.1265	0.5955	0.5956	3.4031	3.4032
	1.5	0.2226	0.2226	0.3330	0.3330	2.5448	2.5449
	2.0	0.3571	0.3572	0.2059	0.2059	2.0011	2.0012
20	0	0.0480	0.0480	1.6685	1.6686	5.7275	5.7275
	0.5	0.0527	0.0527	1.5076	1.5077	5.4443	5.4444
	1.0	0.0668	0.0668	1.1694	1.1694	4.7948	4.7948
	1.5	0.0903	0.0903	0.8511	0.8511	4.0905	4.0906
	2.0	0.1231	0.1231	0.6163	0.6163	3.4808	3.4808
50	0	0.0476	0.0476	1.6850	1.6850	5.7653	5.7653
	0.5	0.0483	0.0483	1.6567	1.6567	5.7167	5.7167
	1.0	0.0506	0.0506	1.5773	1.5773	5.5779	5.5779
	1.5	0.0543	0.0543	1.4605	1.4605	5.3676	5.3676
	2.0	0.0595	0.0595	1.3234	1.3234	5.1094	5.1094
100	0	0.0475	0.0475	1.6874	1.6874	5.7708	5.7708
	0.5	0.0477	0.0477	1.6802	1.6802	5.7585	5.7585
	1.0	0.0483	0.0483	1.6590	1.6590	5.7221	5.7221
	1.5	0.0492	0.0492	1.6249	1.6249	5.6630	5.6630
	2.0	0.0505	0.0505	1.5795	1.5795	5.5832	5.5832